

Accepted Manuscript

Neuronal distribution of *Spatial* in the developing cerebellum and hippocampus and its somatodendritic association with the kinesin motor KIF17

Magali Irla, Murielle Saade, Carla Fernandez, Lionel Chasson, Genevieve Victorero, Nadia Dahmane, Genevieve Chazal, Catherine Nguyen

PII: S0014-4827(07)00427-2
DOI: doi: [10.1016/j.yexcr.2007.09.006](https://doi.org/10.1016/j.yexcr.2007.09.006)
Reference: YEXCR 7609

To appear in: *Experimental Cell Research*

Received date: 11 March 2007
Revised date: 3 September 2007
Accepted date: 5 September 2007



Please cite this article as: Magali Irla, Murielle Saade, Carla Fernandez, Lionel Chasson, Genevieve Victorero, Nadia Dahmane, Genevieve Chazal, Catherine Nguyen, Neuronal distribution of *Spatial* in the developing cerebellum and hippocampus and its somatodendritic association with the kinesin motor KIF17, *Experimental Cell Research* (2007), doi: [10.1016/j.yexcr.2007.09.006](https://doi.org/10.1016/j.yexcr.2007.09.006)

This is a PDF file of an unedited manuscript that has been accepted for publication. As a service to our customers we are providing this early version of the manuscript. The manuscript will undergo copyediting, typesetting, and review of the resulting proof before it is published in its final form. Please note that during the production process errors may be discovered which could affect the content, and all legal disclaimers that apply to the journal pertain.

Neuronal distribution of *Spatial* in the developing cerebellum and hippocampus and its somatodendritic association with the kinesin motor KIF17

Magali Irla^{1,*}, Murielle Saade^{1,*}, Carla Fernandez^{2,&}, Lionel Chasson³, Geneviève Victorero¹, Nadia Dahmane^{2,#}, Geneviève Chazal^{2,4,*}, § and Catherine Nguyen^{1,*}

¹INSERM-ERM206, laboratoire TAGC, Case 928, Parc Scientifique de Luminy, 13288 Marseille Cedex 9, France.

²NMDA UMR 6156, Institut de Biologie du Développement de Marseille, Case 907, Parc Scientifique de Luminy, 13288 Marseille Cedex 9, France.

³CNRS: UMR6102 – INSERM: U631 Centre d'Immunologie de Marseille-Luminy, case 906 Parc Scientifique de Luminy 13288 Marseille, Cedex 9.

⁴Present address : Institut de Neurobiologie de la Méditerranée, Parc Scientifique de Luminy 13288 Marseille, Cedex 9.

‡: Present address: Department of Pathology and Immunology, University of Geneva Medical School, Centre Medical Universitaire, 1 Rue Michel Servet, CH-1211, Geneva, Switzerland.

&: Present address: Laboratoire de Biopathologie de l'Adhésion et de la Signalisation, EA 3281, Faculté de Médecine, 27 Boulevard Jean Moulin, 13385 Marseille Cedex 05.

#: Present address: The Wistar Institute, 3601 Spruce Street, Philadelphia PA19104, USA.

*These authors contributed equally to this work

§ Author for correspondence (e-mail: chazal@inmed.univ-mrs.fr)

Keywords: Spatial gene; development; cerebellum; hippocampus; kinesin motor KIF17

Abstract

We identified the Spatial (Stromal Protein Associated with Thymii and Lymph-node) gene from an adult thymus mouse library of cDNA clones. By RT-PCR, we reported that Spatial was highly expressed in restricted areas of the central nervous system. Here, we characterize the precise cellular localization of Spatial during mouse brain development in the cerebellum, hippocampus and cortex. Five different transcript isoforms have been described for Spatial and among those, only Spatial- ϵ and $-\beta$ present a tightly controlled expression. In the cerebellum, Spatial expression is detected in the external precursor granular layer and persists as these cells migrate and differentiate to form the internal granular layer. It is also expressed in differentiating Purkinje cells with a specific somatodendritic distribution. Spatial expression in the hippocampus is spatially and temporally regulated: it is first expressed in the CA3 field, then in CA1 and later in the dentate gyrus. Interestingly, Spatial- β expression tightly overlaps with the beginning of neuronal differentiation in both structures. Using cultured hippocampal neurons, we show that Spatial also exhibits a somatodendritic distribution and it is concentrated in some synaptic regions. Moreover, the vesicle-like cellular distribution of Spatial protein in dendrites is similar to that described for the kinesin motor protein KIF17. Immunofluorescence analyses show that Spatial co-localizes with KIF17 in dendrites of hippocampal neurons in primary culture. Additionally, co-immunoprecipitation experiments of endogenous proteins from hippocampus confirmed that Spatial and KIF17 physically interact. These findings suggest that Spatial may play a role in neuronal morphogenesis and synaptic plasticity through its interaction with the kinesin motor KIF17 in dendrites.

Introduction

During development, organ differentiation occurs through a tight regulation of specific genes. Most of these developmental genes are common to different organs. Indeed, it is known that molecules, considered characteristic of one system, are used by another as signalling substances. For instance, cytokines in the thymus are implicated in thymocyte maturation and, in the brain, are necessary for the development and differentiation of neurons [1].

Using DNA chip technology we isolated the *Spatial* (Stromal Protein Associated with Thymic and Lymph-node) gene by an approach based on differential screening between different knock-out mice models exhibiting distinct thymic immunodeficiencies. This analysis led to the identification of three adult variants of the *Spatial* gene expressed in the thymus (GenBank accession nos. AF257502, AF257503 and AY243457) [2, 3]. In addition, we also described two other isoforms isolated in the testis (GenBank accession no. AF521592 and AF521591) [4]. According to the size of alternative spliced variants, we have respectively named Spatial isoforms: Spatial- α (1035 bp), Spatial- β (1002 bp), Spatial- γ (933 bp) for short isoforms identified in the thymus and Spatial- δ (1353 bp) and Spatial- ϵ (1454 bp) for the long isoforms identified in the testis [3]. Thus, this gene generates at least five alternative spliced variants: three short isoforms (Spatial- α , - β and - γ) and two long isoforms (Spatial- δ and - ϵ) with a tissue-specific distribution [3, 4]. These isoforms do not exhibit obvious structural or protein homologies conserved with well defined protein families [3, 5]. Thus, the biological function of *Spatial* remains completely unknown. In the adult mouse thymus, *Spatial* is expressed in the subcapsular region, which is made up of polarized epithelial cells [2]. In the adult mouse testis, *Spatial* is a postmeiotic gene associated with drastic morphological changes of germ cells [5]. More specifically, in round spermatids, its distribution strongly correlates with the formation of the nascent flagellum and during the elongation process, with the manchette involved in the shaping of the nucleus. Thus, *Spatial* is closely correlated with spermatid differentiation. Besides its expression in the thymus and the testis, analysis by RT-PCR of a wide panel of mouse tissues showed that *Spatial* is also expressed in the central nervous system (CNS) more particularly in the cerebellum and hippocampus as well as to a lower extent in the cortex [4].

Interestingly, fundamental homologies in (1) the structural microenvironment between the brain and the thymus [1] and in (2) migration and differentiation processes between the testis and some compartments of the nervous system suggest that certain mechanisms and pathways are

conserved between these organs. We also showed that Spatial interacts with kinesin KIF17b, a testis-specific isoform of the brain kinesin-2 motor protein KIF17 [5, 6]. This interaction is restricted to highly organized cytoskeletal structures such as the manchette and the principal piece of the sperm tail. Although the role of KIF17b in these structures is still unknown, the function of the kinesin-2 motor KIF17 in other highly organized cytoskeletal structures, such as the cilia and dendrites, has been well established [7-9]. Indeed, KIF17 was shown to transport organelles, vesicles, channels, protein complexes and RNA to specific subcellular compartments in neurons [7-10]. These results raise the possibility that Spatial may also interact with KIF17 during brain development.

Here, we describe a detailed characterization by quantitative RT-PCR and Western blot analyses of the expression of different Spatial isoforms which exhibit a developmental and tissue-specific distribution. In the developing cerebellum, Spatial is expressed by both granule and Purkinje neurons. In the hippocampus, we show that Spatial is sequentially expressed in the CA3 and CA1 areas and later in the dentate gyrus. Using markers of specific subcellular compartments in neurons, we show both *in vivo* and *in vitro* that Spatial is likely to act in the somatodendritic region of neurons rather than in axons. We also demonstrate that Spatial proteins appear in some synaptic regions as identified by the synaptophysin marker. Finally, we show that Spatial and KIF17 interact physically *in vivo* and that they co-localize in dendrites of cultured hippocampal neurons. Our results suggest that Spatial may be involved in cerebellar and hippocampal development affecting neuronal differentiation, morphogenesis and synaptic plasticity.

Materials and methods

Animals

All analyses were performed on C57BL/6 mice maintained under specific-pathogen free conditions. Mouse embryos were staged counting the morning after conception as embryonic day (E) 0.5. Embryos were analyzed starting day E16. Adult mice were used between 6 and 8 weeks of age. All experimental and surgical procedures were approved by the veterinary office of the Ministry of Agriculture, France (authorization number: 13–27).

***In situ* hybridization**

In situ hybridization was carried out on E16 mouse embryos that were fixed by immersion overnight in 4% paraformaldehyde (Sigma Aldrich). Postnatal and adult brains were fixed by perfusion with 4% paraformaldehyde and post-fixed for 4 h at 4°C. The Spatial cDNA fragment (1.3 kb) was subcloned into the pGEM-T vector (Promega). Sense and antisense riboprobes were prepared by *in vitro* transcription using T7 and SP6 polymerases, respectively, with digoxigenin-UTP (Boehringer Mannheim). The *in situ* hybridization of sections was performed using a standard protocol [11]. Then, sections were counterstained with hematoxylin (Sigma Aldrich) to localize transcript expression. Images were taken using Zeiss, axiophot 2 microscope with Nikon digital camera DXm1200.

Quantitative TaqMan RT-PCR

Quantitative RT-PCR was performed on the cerebellum and the hippocampus at different stages of development to evaluate the distribution of short and long Spatial isoforms by using the ABI PRISM 7000 Sequence Detection System. Random hexamers and the TaqMan reverse transcription reagents from the RT reaction mix (Applied Biosystems) were used to reverse transcribe total RNA. The PCR step was performed with TaqMan universal PCR master Mix and assays-on-demand gene expression probes (Applied Biosystems). Primers and the TaqMan probe used to detect specifically short isoforms were: forward primer: 5'-TTGGAACCAGCCCCTGTTT-3', reverse primer 5'-GTTCTCCGGCTTCGTCTCT-3' and FAM 5'-CCTTTGGACTAGTCACCTCAT-3' NFQ. Primers and the TaqMan probe used to detect specifically long isoforms were: forward primer: 5'-GCTTCAAGAGCC TCAAGAGACA-3', reverse primer 5'-GGTGGTGACCTAGTCTTCTTCAG-3' and FAM 5'-ACTGTAGGCTGCCTCTTG-3' NFQ. The 18S-rRNA was amplified from all samples on each plate as a housekeeping gene to normalize expression between different samples and to monitor assay reproducibility. A non-template control was included for each target analyzed. Relative quantification of all targets was calculated by using the comparative cycle threshold method [12].

Western blot

Proteins were extracted by using the Nuclear Protein Extraction Kit (Panomics). Protein concentrations were measured using the Pierce BCA protein assay. Protein samples were run on SDS-polyacrylamide gel (Invitrogen) and transferred to nitrocellulose membranes (BioRad).

Incubation with the purified Spatial polyclonal antibody (1:2000) was performed overnight at 4°C. This antibody was produced by immunizing rabbits against the mouse recombinant 6×His-Spatial- α protein that shares a conserved sequence with all Spatial isoforms and further purified on a protein G column (Eurogentec). Mouse polyclonal anti- β -actin was used as loading control (Santa Cruz Biotechnology). The anti-KIF17 antibody (clone M-20) was purchased from Santa Cruz Biotechnology. Proteins were visualized using horseradish peroxidase-conjugated secondary antibody (1:1000; Amersham Pharmacia Biotech) and the enhanced chemiluminescence (ECL) detection system (Pierce).

Two-dimensional gel analysis

Two dimensional electrophoresis was done according to the method of O'Farrel using an immobilized pH gradient system (IPG-PHOR, Pharmacia Biotech) [5]. Seven cm strips were rehydrated 12 h in 8 M urea, 2 % (w/v) CHAPS, 0.5 % (v/v) IPG buffer, 2.8 mg/ml DTT and bromophenol blue containing 300 μ g of adult cerebellum protein extracts. The isoelectric focusing was performed at 500 V for 30 min, 1000 V for 30 min and 8000 V for 1 h, over a pI linear range of 3 to 10. SDS-PAGE was performed according to the method of Laemmli using 10 % (w/v) slab gels (PROTEAN II, Bio-Rad laboratories) [13]. Proteins were separated in a second dimension following their molecular mass using constant voltage of 160 V at 20°C. The migrated proteins were detected by Coomassie staining. Standard proteins were used to calculate molecular weight and pI values.

Immunofluorescence

Mice of different ages and pregnant female were deeply anaesthetized with a mixture of Rompun/Imalgen 500 and intracardially perfused with a solution of 4% paraformaldehyde (PFA) in PBS, pH 7.2. Brains were dissected out, post-fixed for 48 h in 4% PFA at 4°C, and then stored in PBS. Immunofluorescence was performed on floating sections. Serial sagittal sections of 50 μ m were performed with a Vibratome (Leica). Sections were first incubated for 2 h at room temperature with DMEM 10% FCS (Fetal Calf Serum) to reduce non-specific labeling. Then, they were incubated overnight at 4°C with Spatial polyclonal antibody (1:100), synaptophysin (SY38 1:10, Chemicon), MAP2 (clone HM-2; 1:500; Sigma), KIF17 (clone M-20; 1:200), antiphosphorylated NF-H (clone SMI31; 1:300, Chemicon) or GFAP (clone G-A-5; 1:200,

Sigma) antibodies. They were then washed in PBS before incubation with the corresponding Alexa fluorescent secondary antibodies (Molecular Probes) for 45 min at room temperature. Sections were counterstained with 4', 6'-diamidino-2-phenylindole (DAPI) at 1 µg/ml for 5 min at room temperature (Calbiochem) and mounted with Mowiol fluorescent mounting medium (Calbiochem). Controls were performed either by omitting the first antibody or by replacing the first antibody with a non-immune serum. Fluorescent images were acquired with the Zeiss LSM 510 confocal microscope. Raw images were processed only for intensity and contrast adjustments using LSM 5 Image browser.

Immunoprecipitation

To prepare resin immobilized antibodies, polyclonal antibodies for Spatial and control IgG (20 µg) were diluted with coupling buffer (0.1 M NaHCO₃ buffer containing 0.5 M NaCl, pH 8.3) and were incubated with cyanogen-bromide activated resin for 4 h (Sigma). Unreacted ligand was washed away with the coupling buffer and resin unreacted groups were blocked with 0.2 M glycine, pH 8.0 for 2 hours. The resin was then washed extensively to remove the blocking solution, first with basic coupling buffer, then with acetate buffer 0.1 M, pH 4.0 containing 0.5 M NaCl. This wash cycle of high and low pH solutions was carried out 3 times. For immunoprecipitation, mouse hippocampal extract (1 mg) was incubated overnight with resin immobilized antibodies in a final volume of 1 ml of immunoprecipitation buffer (TBS, 0.1% Tween 20) in the presence of proteinase inhibitor mixture (Sigma). The resin was then collected by centrifugation at 2000 g for 30 sec. and washed four times with 1 ml of immunoprecipitate buffer. To recover precipitated proteins, the resin was resuspended overnight at 4°C in 20 µl of SDS gel loading buffer without β-mercaptoethanol to not disturb the structure of the antibody. After a brief spin, the supernatant was collected and boiled for 5 min with SDS gel loading buffer containing β-mercaptoethanol and proteins were separated by 10% SDS-polyacrylamide gels (Invitrogen). For immunoprecipitation with KIF17 antibody, the resin was replaced by 50 µl of protein G-agarose beads (Zymed Laboratories) and precipitated proteins were treated with the same washes with TBS, 0.1% Tween 20 and elution with SDS gel loading buffer containing β-mercaptoethanol as mentioned above.

Primary cultures of mouse hippocampal neurons

The hippocampal formation was dissected from 16 to 18 days mouse brain embryos and dissociated using trypsin (Invitrogen). Dissociated cells were plated on coverslips (Marienfield) coated with poly-L-lysine (Sigma, 0,1 mg/ml) at a density of 70 000 cells/cm in minimal essential medium (MEM) supplemented with 10% NU serum (BD Biosciences), 0.8% glucose, 1mM sodium pyruvate, 2mM L-Glutamine, and 10 IU/ml penicillin–streptomycin. On days 7, 10 and 13 of culture incubation, one-half of the medium was changed to MEM with 2% B27 supplement (Invitrogen). Immunohistochemistry was performed as already described using anti-MAP2 (clone HM-2; 1:500; Sigma), anti-phosphorylated NF-H (SMI31, 1:500, Sigma) and anti-synaptophysin (SY38 1:10, Chemicon).

Results

Spatial- ϵ and - β isoforms are differentially expressed during cerebellar development

In order to define the precise expression pattern of *Spatial*, we performed *in situ* hybridization (ISH) analyses at different stages of cerebellar development using a probe that detects all isoforms (Figs. 1A-E). *Spatial* mRNA expression was analyzed at embryonic day 18 (E18) where it is detected in granule cell precursors (GCPs) located in the external granular layer (EGL) (Fig. 1A, arrow). This expression is stronger in the anterior side of the cerebellum and this differential expression is maintained up to early postnatal stages (P0-P3, Figs. 1B,C). At later stages of postnatal development, the newly post-mitotic granule cells leave the EGL and migrate inwards to form the internal granular layer (IGL) where granule neurons terminally differentiate. At P8, the expression of *Spatial* is still strong in the EGL but begins to be observed in the IGL (Fig. 1D, asterisk). In the adult cerebellum, *Spatial* is strongly expressed by granular cells of the IGL (Fig. 1E1). Furthermore, at higher magnification we found that in addition to granular cells (Fig. 1E2, asterisk), *Spatial* is also expressed although at lower levels, by Purkinje cells (Fig. 1E2, encircled regions). Together these results show that in addition to Purkinje cells, *Spatial* is expressed by granule cells as they proliferate, migrate and differentiate.

In order to precisely determine the expression profile of long and short isoforms of the *Spatial* gene during cerebellar development, we performed a quantitative TaqMan RT-PCR at different stages of development from E18 to the adult stage (Fig. 1F,G). The expression of *Spatial*

isoforms was measured relative to the expression of the housekeeping 18S-rRNA gene. Long isoforms are detected at similar levels between E18 and P3 stages (Fig. 1F). At P8, this expression increases approximately 8-fold and then decreases to reach a basal level in the adult. In contrast, short isoforms are weakly expressed between E18 and P3 stages and then this expression is increased and maintained at later stages of development to reach a plateau in the adult (Fig. 1G). Altogether, this analysis shows a differential expression between the long and short isoforms suggesting a different function at different times of cerebellar development.

We next investigated which isoforms of the Spatial protein are expressed in the cerebellum. We examined the expression of Spatial in the adult cerebellum using two-dimensional SDS-PAGE. To detect Spatial proteins, we used after Western blot the polyclonal anti-Spatial antibody generated in our laboratory against all Spatial protein isoforms [3-5]. Two proteins at 52 kDa and 34 kDa were detected, corresponding respectively to the Spatial- ϵ long isoform with an isoelectric point (pI) of around 6.5 and the Spatial- β short isoform with a pI of around 9.00 (Fig. 1H). This result is consistent with previous bioinformatic analyses showing the biochemical properties of the different Spatial isoforms [3].

We further studied the protein expression pattern of Spatial isoforms by Western blot during mouse cerebellar development (Fig. 1I). Two major cross-reactive proteins were also observed at 52 and 34 kDa corresponding to Spatial- ϵ and - β respectively, which is consistent with the two-dimensional SDS-PAGE result. Quantitative analysis of the blot indicated that the level of Spatial- ϵ protein gradually increases from early stages of development (E18-P0) to adult while the Spatial- β isoform is detected later, around P3 and becomes stronger at P30 (Supplementary data, Fig. 1). In addition, the expression of these two isoforms is maintained in the adult. None of these proteins is detected with the pre-immune serum confirming the specificity of the antibody (data not shown, [5]). Thus, Spatial- ϵ and - β isoforms are differentially expressed during cerebellar development and the temporal protein expression pattern of these isoforms strongly correlates with their respective mRNA levels.

Spatial is expressed in the somatodendritic compartment of Purkinje cells and in glomeruli of the IGL

To confirm ISH observations and specify the subcellular localization of Spatial proteins during cerebellar formation, immunofluorescence analyses were performed using the anti-Spatial

polyclonal antibody (Fig. 2). As previously observed by ISH, *Spatial* is strongly expressed in the EGL at P8 (Fig. 2A, arrow). At higher magnification, we observed that *Spatial* is not only expressed by mitotically active cells forming the outer EGL [11] but also by Purkinje cells (Figs. 2B1,B2, encircled regions) and granule cells of the developing IGL (Fig. 2B, asterisk). A costaining with a GFAP antibody (Fig. 2C1) shows that *Spatial* is restricted to neurons as it is not expressed in GFAP positive structures (see higher magnification in Fig. 2C2). At this stage of development, *Spatial* is also detected in cell bodies of Purkinje cells not yet well aligned as in the adult (Fig. 2D1, arrowheads). To highlight the subcellular localization of *Spatial* in the developing IGL and determine whether it is localized in glomeruli structures composed of synaptic terminals, we performed a co-staining analysis using synaptophysin as a glomeruli marker (Fig. 2D2-D4). As shown in figure 2D4, (higher magnification of the box in D3), *Spatial* is detected in granule cell bodies in the forming IGL (arrow) and also in the synaptophysin positive glomeruli structures (asterisk)[14].

Additionally, we have carefully characterized the expression of *Spatial* protein in the adult cerebellum, where it is strongly expressed in the IGL and Purkinje cells, which is consistent with the ISH results (Fig. 2E1-G4). To highlight the subcellular localization of *Spatial* in these neurons, the MAP2 dendrite marker, and the neurofilament (NF) axonal marker, were used [3]. In Purkinje neurons, *Spatial* is detected in the elaborate dendritic trees specifically identified by MAP2 (Figs. 2E1-E4). In contrast, *Spatial* is not expressed in axon of Purkinje cells since no co-localization with the NF marker was observed (Figs. 2F1-F4). In the IGL, *Spatial* is expressed in the differentiated granule cells and concentrated in glomerular synaptic structures detected with the synaptophysin marker (Figs. 2G1-G4). However, *Spatial* and synaptophysin signals do not overlap, as they are clearly distinguishable as shown in the Fig. 2G4. Similar results were obtained with the GABA α - receptor of the major inhibitory neurotransmitter in the CNS, which also labels these glomerular structures (data not shown). Altogether, these results show that *Spatial* is expressed exclusively in dendritic extensions of Purkinje neurons and in glomerular structures of granule neurons in the IGL.

Spatial presents a differential distribution during hippocampal development

During the development of the CNS, *Spatial* mRNA expression is also detected in the hippocampal formation (Fig. 3). At E16, its expression is restricted to the CA3 layer (Fig. 3A).

Then, starting at P0, a weak expression is observed in the CA1 layer (Fig. 3B) and at P8, *Spatial* is detected in the entire hippocampal formation: in CA3 and CA1 pyramidal layers and the dentate gyrus (Fig. 3C). The same expression pattern is conserved at adult stage (data not shown). Quantitative TaqMan RT-PCR analysis at different stages of development (E16 to P8) showed that both the long and short isoforms are expressed (Fig. 3D). The expression of long isoforms does not vary significantly until P0 and then it slightly increases at P8. In contrast, short isoforms are expressed at E16 and P8 but not detected at P0. We further characterized the expression of *Spatial* protein isoforms by Western blot from E16 to P8 stages (Fig. 3E). The *Spatial*- ϵ long isoform is detected at E16 and P0 and its expression significantly increases at P8. In addition to *Spatial*- β , the *Spatial*- γ short isoform is also detected at E16 and P8 stages in contrast to P0 stage where only a faint signal is observed. However, these two short isoforms were detected at lower levels than those observed for the *Spatial*- ϵ long isoform. Thus, as in the cerebellum, the protein expression pattern of *Spatial* is consistent with the quantitative RT-PCR analysis.

Thereafter, we determined by immunofluorescence analyses the distribution of *Spatial* proteins in the hippocampus at the adult stage (Fig. 4). We found that *Spatial* is strongly expressed in the three regions of the hippocampal formation (CA3, CA1 and dentate gyrus) (Fig. 4A) as shown by ISH. *Spatial* proteins are specifically detected in the cytoplasm and dendritic processes of both CA3 (Fig. 4B) and CA1 (Fig. 4C) pyramidal cells. We further confirmed this somatodendritic distribution of *Spatial* proteins *in vivo* in the CA3 pyramidal cells by co-staining with the MAP2 marker (Figs. 4D1-D3). The same distribution was also observed in CA1 pyramidal cells (data not shown). Moreover, as described at P8, *Spatial* expression is restricted to neurons as no co-localization of *Spatial* with glial markers such as GFAP (Figs. 4E1-E3) and Galc was observed *in vivo* (data not shown). Next, we analyzed the distribution pattern of *Spatial* in the synaptic regions by a co-immunostaining with anti-*Spatial* and anti-synaptophysin antibodies (Figs. 4F1-F3). At high magnification, we observed that *Spatial* proteins are localized in some synaptic regions (in the box).

In the dentate gyrus, we observed dramatic changes in *Spatial* expression during its development. At P16, the most superficially located granular cells strongly express *Spatial*. This external layer is composed of differentiated granule cells where *Spatial* exhibits a somatodendritic distribution (Figs. 4G1-G3, arrow). In contrast, cells proliferating in the subgranular layer located in the inner side do not express *Spatial* (Figs. 4 G1-G3, asterisk). In the adult, all granule cells of the dentate

gyrus continue to express Spatial (Figs. 4H1-H3).

We further confirmed the restricted somatodendritic pattern of Spatial *in vitro* on cultured hippocampal neurons. Spatial proteins were also shown to be tightly co-localized with MAP2 in the somatodendritic compartment of hippocampal pyramidal cells (Figs. 5 A1-A3). In contrast, mainly no colocalization was observed with the NF (SMI31) axonal marker showing that Spatial is not a specific marker of axonal processes (Figs. 5 B1-B3). We further investigated the presence of Spatial proteins in synaptic compartments on cultured hippocampal neurons by using the synaptophysin marker (Figs. 5 C1-C3). At high magnification, we observed that Spatial proteins are concentrated in some synaptic regions (Figs. 5 D1-D3, arrowheads).

Altogether, these data show that Spatial exhibits a somatodendritic distribution in pyramidal cells of CA3 and CA1 layers as well as in differentiating granule cells in the dentate gyrus and it is present in some synaptic regions.

Spatial association with the kinesin motor KIF17

In addition to its distribution in dendrites restricted to specific neuronal cell types in the CNS, Spatial is also expressed in the spermatozoa flagellum [5]. Dendrite and flagella share similar molecular motor components which are proposed to mobilize cargo proteins along microtubules [15]. One of these molecular motors is the kinesin KIF17 known to transport neuronal proteins to dendrites [15, 16]. The KIF17 testis specific isoform, kinesin KIF17b [6], associates with Spatial- ϵ isoform in highly organized cytoskeletal arrays in the manchette as well as the spermatozoa flagellum [5]. In order to determine if an interaction between Spatial and KIF17 is also present in the CNS, we performed immunoprecipitation experiments using mouse hippocampal proteins (Fig. 6A). We found that the anti-Spatial antibody coimmunoprecipitates KIF17 with the Spatial- ϵ and - β as predicted (Fig. 6A, left panel) while control IgGs do not. This result indicates that Spatial and KIF17 physically interact *in vivo*. To further investigate this interaction and determine the specificity of Spatial isoforms in the KIF17 interaction, co-immunoprecipitation of endogenous proteins from total hippocampus extracts was performed with anti-KIF17 antibody (Fig. 6A, right panel). These experiments showed that anti-KIF17 antibody efficiently immunoprecipitates Spatial- ϵ and - β . Thus, these results suggest that KIF17 interacts with the

Spatial- ϵ and - β in the hippocampus *in vivo*.

Next, we studied whether Spatial and KIF17 co-localize in similar structures using primary cultures of hippocampal neurons (Fig. 6B). Double staining with the anti-KIF17 and anti-Spatial antibodies showed a co-localization of these proteins in a vesicle-like distribution in dendrites. At higher magnification, the majority of punctate vesicles labeled with anti-Spatial antibody co-localize with anti-KIF17b labeling. We further investigated the association between these two proteins *in vivo* by immunofluorescence on brain sections (Figs. 6C-D). As previously shown, KIF17 has been detected in abundance in the gray matter, especially in pyramidal cells of the hippocampus [9]. Interestingly, in the hippocampal CA3 region, we observed at high magnification that the characteristic vesicle-like profile staining obtained with the anti-KIF17 antibody colocalizes with Spatial proteins (Fig. 6C).

In addition to the cerebellum and hippocampus, Spatial was also observed in the cerebral cortex where KIF17 is also specifically expressed (Supplementary data Fig. 2) [9]. Interestingly, we observed that Spatial and KIF17 also co-localize in this brain area (Fig. 6D). Altogether, co-immunoprecipitation and co-staining analyses demonstrate that Spatial and KIF17 physically interact in the brain.

Discussion

The Spatial gene generates at least five alternative spliced variants: three short isoforms (Spatial- α , - β and - γ) and two long isoforms (Spatial- ϵ and - δ) with a tissue specific distribution [3]. This gene is expressed in highly polarized cell types, such as epithelial cells in the thymus, germ cells in the testis and neurons in the brain. Although its biological function remains unknown, its unique distribution suggests that it may be involved in cell morphogenesis. Indeed, we recently showed that in the testis, Spatial proteins are distributed in highly organized cytoskeletal structures surrounding the nascent flagellum and in the manchette during spermatids differentiation [5]. We provided first evidences of a function of Spatial in spermatid differentiation as a new cargo of kinesin KIF17b, in a microtubule-dependent mechanism specific to the manchette and the principal piece of the sperm tail. In a previous RT-PCR analysis on a wide panel of mouse tissues, we showed that Spatial is also expressed in restricted regions of the CNS, most in the cerebellum and hippocampus [4]. In the present paper, we characterize in detail Spatial expression pattern during the development of the mouse brain.

In the cerebellum, Spatial expression is detected at early stages in immature granule neurons, which are generated in the EGL. At later stages, it is detected in differentiating granule cells migrating through the molecular layer and reaching their destination in the IGL within 4-5 days after their generation. Biochemical analyses showed that only the Spatial- ϵ long isoform is present in these mitotic granule neuron precursors at early stages (E18-P3). Later, when post-mitotic granule cells migrate and differentiate to form the IGL, the expression of Spatial- ϵ persists and the Spatial- β short isoform is induced. Interestingly, the beginning of Spatial- β expression overlaps with the beginning of post-mitotic granule cells differentiation which appears around P4 [17]. Then, Spatial expression appears in the IGL showing its highest expression at P8. In addition, at around P8 Purkinje cells undergoing differentiation also begin to express Spatial proteins in their cell bodies and arborescent dendrites which form the molecular layer [18]. At this stage, the appearance of Spatial expression in the differentiating Purkinje cells coincides with the increase of Spatial- β mRNA levels up to 3.5-fold. All together, these observations suggest that during postnatal development of the cerebellum, the Spatial- β short isoform could play a crucial role during granule and Purkinje neurons differentiation.

During the formation of the hippocampus, Spatial presents a sequential expression in the Ammon's horn and the dentate gyrus. At early postnatal stages, Spatial is expressed in the CA3 and CA1 areas, while from P8 onwards it is also detected in the DG. This sequential expression can be due to the fact that the Ammon's horn develops during embryonic development, between E14 and E16, while the DG starts to be formed around E18 and continue to develop until P20. In the developing DG, the granule cell layer exhibits an "outside-in" gradient of development, with the earliest generated cells found inside and the most mature neurons outside [19]. Proliferating cells in the subgranular layer located on the inner side do not express Spatial. In contrast, Spatial is detected in post-mitotic granule cells that continuously migrate and differentiate into mature neurons to form the superficial granule layer [20]. This particular expression in granule cells during differentiation reinforces the hypothesis that Spatial is involved in neuronal morphogenesis which also continues in the adult [20]. In addition, mRNA and biochemical analyses of Spatial expression during hippocampal development are in agreement with a potential involvement of Spatial isoforms in morphogenesis. Spatial- ϵ expression persists during all developmental stages of the hippocampus. However the developmental pattern of Spatial- β and Spatial- γ short isoforms is correlated with neuronal morphogenesis and neurite formation in this region. For pyramidal cells of Ammon's horn, the highest rate of neurogenesis occurs at late embryonic stages (E14-E16) which correspond to the beginning of Spatial short isoform expression. In granule cells of the dentate gyrus, the highest rate of neurogenesis occurs between P1 and P9 and by P20 this process is nearly complete[19]. Interestingly, it is during this intensive period of neurogenesis that Spatial short isoform is re-expressed. This reappearance of Spatial reinforces the hypothesis that Spatial short isoforms could be involved in neuronal morphogenesis. Using cultured hippocampal neurons, we demonstrated that (1) Spatial exhibits a somatodendritic pattern and (2) is concentrated in some synaptic regions. Moreover, hippocampal CA1-CA3 pyramidal cells, granular DG cells as well as cerebellar granule and Purkinje cells retain high levels of Spatial expression in the adult brain. Therefore, Spatial might also contribute to the synaptic plasticity in these cells enabling long-term potentiation processes such as learning and memory [21, 22]. Receptors and other proteins synthesized in the cell body are often transported to pre/postsynaptic sites by the kinesin superfamily of proteins (KIFs) [23]. KIF17, a homodimeric microtubule anterograde motor protein, when overexpressed, enhances spatial and working memory in mice [9, 24]. Interestingly, Spatial shows the same cellular distribution as

KIF17 which is specific to the grey matter [9]. These two genes are both expressed in the cerebellum, hippocampus, and cerebral cortex. In addition, they are both specifically localized in neuronal dendrites. We identified the Spatial-KIF17 co-localization in dendrites of cultured hippocampal neurons with a punctate and discontinuous staining also shown for other subunit trafficked by KIF17, as glutamate receptors (GluR5) [25] and N-methyl-d-aspartate receptor (NR2B) [26]. We also showed the co-localization of endogenous Spatial and KIF17 in vesicles *in vivo* specifically in the hippocampus and the cerebral cortex. KIF17 is associated with Spatial through interaction with Spatial- ϵ and Spatial- β isoforms. We could expect that Spatial does bind to a KIF17 through a specific motif conserved between these isoforms since the extreme N terminus of Spatial- ϵ and - β shares a sequence (amino acids 19-259) with 70.8% identity. Further studies based on amino acid substitutions in this region will be necessary to find the domain by which Spatial and KIF17 interacts. Moreover, since Spatial short isoform expression overlaps with the start of granule and pyramidal cells differentiation, we can also suggest that Spatial- β could co-assemble with Spatial- ϵ and be transported from the soma to the dendrites in a kinesin dependent fashion to play a role in cell morphogenesis. In addition, a piece of evidence suggests that Spatial- β extension targeting is accomplished through the involvement of Spatial- ϵ since long isoforms contain a particular carboxy-terminal motif (RVHP; amino acids 291-294 for Spatial- ϵ), in fitting with the RVxP motif, involved in the extension localization of some proteins. For instance, in the case of the cyclic nucleotide-gated (CNG) channels subunit, CNGB1b, that interacts with KIF17 in olfactory sensory neurons [7], it was shown that both the RVxP motif of CNGB1b and KIF17 interaction are required for ciliary targeting of these protein channels. Additional experiments based on (1) amino acid substitutions in this motif and (2) KIF17b inhibition are required in order to demonstrate the mechanisms for Spatial extension targeting. In conclusion, we report Spatial expression in the CNS and more specifically during the development of the mouse cerebellum and hippocampus. Although Spatial short isoforms are likely to play a role in neuronal morphogenesis through the formation of a Spatial- β - ϵ /KIF17 complex, defining how KIF17 could contribute and modulate the localization and activity of Spatial in the CNS needs to be further investigated.

Acknowledgments

We thank Christophe Pellegrino (INMED, Marseille, France), Renaud Vincentelli (CNRS, UMR 6098, Marseille, France) and Florence Goulhen (CNRS-IBSM, Marseille, France) for technical helps. We also acknowledge Dr Fiona Francis (INSERM U106, Paris, France) and Dr Marie-Claude Potier (UMR7637, Paris, France) for critical reading of the manuscript. Immunofluorescence experiments were done with the facilities of the murine genomic platform of the Marseille Nice-genopole. This work was supported by the Institut National de la Santé et de la Recherche Médicale (INSERM). Magali Irla is supported by a fellowship from l'Association pour la Recherche sur le Cancer (ARC) and Murielle Saade is supported by a grant from the INSERM Provence-Alpes-Côte d'Azur région.

ACCEPTED MANUSCRIPT

Legends

Fig. 1- Spatial expression during cerebellar development. (A-E) Spatial is predominantly expressed by granule cells during cerebellar development. Mouse embryonic (E18), postnatal (P0, P3, P8) and adult cerebellar sagittal sections were hybridized with an antisense *Spatial* riboprobe. (A-D) Spatial expression is detected at late embryonic (E18) and postnatal stages in the EGL as indicated by the arrow. (A-C) From E18 to P3, *Spatial* is expressed in a gradient along the anterior-posterior axis, being more strongly expressed in the anterior part of the cerebellum. At P8, *Spatial* is more uniformly expressed along the entire EGL and starts to be expressed in the forming IGL (asterisk, D). In the adult, *Spatial* expression is observed in granule cells within the IGL (E1). The panel E2 represents a higher magnification of the expression pattern observed in the IGL at the adult stage (asterisk) and in Purkinje cells (circled cells). Scale bars in (A-E1): 400 μm ; (E2): 20 μm . (F, G) *Spatial* isoforms are differentially expressed during mouse cerebellar postnatal development. Quantitative TaqMan RT-PCR analysis was performed for long and short *Spatial* mRNAs during mouse postnatal cerebellum development. In each stage, the expression level of cDNAs was normalized to the expression level of the housekeeping gene 18S-rRNA. The ratios of long and short *Spatial* mRNAs/18S-rRNA from each stage were standardized to *Spatial* expression in the adult (Ad.) which was considered as 1. (H) Western blot analysis of two-dimensional SDS-PAGE of *Spatial* from adult cerebellum extracts reveals *Spatial*- ϵ (pI 6.5, MW 52 kDa) and *Spatial*- β (pI 9, MW 34 kDa) isoforms. (I) Western blot analysis performed on mouse cerebellum extracts from different stages of postnatal development revealed two proteins at 52 and 34 kDa corresponding to *Spatial*- ϵ and - β , respectively.

Fig. 2- Tissular and subcellular localization of *Spatial* proteins during cerebellum development. (A-D4) Cerebellar sagittal sections at P8 stage were immunostained with the anti-*Spatial* antibody. (A) *Spatial* is strongly detected in the EGL and more weakly in the forming IGL. (B) Higher magnification of the right lower box in A shows that *Spatial* is expressed in cell bodies of mitotic granule cells of the EGL (arrow), Purkinje cells (encircled areas) and granule cells of the IGL (asterisk). (C1,C2) Double immunostaining with anti-*Spatial* and anti-GFAP antibodies shows that *Spatial* does not colocalize with the GFAP astrocytes marker. C1 is a higher magnification of the same area as the upper left square in Fig. 2A. C2 is a higher magnification of

the square in C1. D1-D3 shows the staining of Spatial and the synaptic vesicle marker synaptophysin. (D4) This higher magnification shows the expression of Spatial in cerebellar glomeruli stained with the synaptophysin marker (asterisk) and the cytosolic localization of Spatial proteins in granule cells (arrow). (E1-G4) Adult cerebellar sections were immunostained with the anti-Spatial antibody. (E1-E4) Co-immunostaining of Spatial and the dendritic marker MAP2 shows that Spatial is expressed in the elaborate dendritic tree of Purkinje cells (E4, higher magnification of the area boxed in E3). In contrast, co-immunostaining of Spatial and the axonal marker neurofilament (NF) shows that Spatial is not expressed in axonal processes of Purkinje cells and granule cells of the IGL (F1-F3; F4: higher magnification of the box in F3). (G1) Co-immunostaining of Spatial and the synaptic synaptophysin marker. (G2-G4) A higher magnification of the IGL shows the expression of Spatial in glomeruli structures (arrowheads). Cells nuclei are visualized by a DAPI counterstaining. Scale bars in (A): 200 μm ; (B): 50 μm ; (C1): 25 μm ; (C2): 10 μm ; (D1-D3): 20 μm ; (D4): 10 μm ; (E1-E3): 50 μm ; (E4): 10 μm ; (F1-F3): 100 μm ; (F4): 30 μm ; (G1): 50 μm and (G2-G4): 20 μm .

Fig. 3- Spatial displays a sequential distribution during perinatal development of the hippocampus. (A-C) Spatial expression was analyzed by ISH on mouse brain sagittal sections at E16, P0 and P8 stages. (A) Spatial expression is first detected in the CA3 layer at E16. (B) At P0, it is also observed in the CA1 layer and at P8, Spatial is strongly expressed in the dentate gyrus (DG) and then in the entire hippocampal formation (C). Scale bars in (A, B): 100 μm ; (C): 400 μm . (D) Quantitative TaqMan RT-PCR analysis was performed for long and short Spatial mRNAs during mouse hippocampus development. In each stage, the expression level of cDNA was normalized to the expression level of the housekeeping gene 18S-rRNA. The ratios of long and short Spatial mRNAs/18S-rRNA from each stage were standardized to the E16 stage Spatial expression which was considered as 1. (E) Western blot analysis performed on mouse hippocampus extracts prepared at different stages of development, revealed three proteins at 52, 34 and 32 kDa corresponding to Spatial- ϵ , - β and - γ , respectively.

Fig. 4- Spatial displays a somatodendritic localization in the hippocampal neurons of the CA3, CA1 and DG layers. (A) Immunofluorescence analysis on adult brain sections showed that Spatial proteins are expressed both in the CA3 and CA1 layers, in addition to the DG. (B,C) At

higher magnification, Spatial staining is visible in the cytoplasm and processes of the CA3 and CA1 pyramidal cells. (D1-D3) A double immunostaining with anti-Spatial and anti-MAP2 antibodies shows that Spatial colocalizes with the MAP2 somatodendritic marker in the CA3 area. (E1-E3) A double immunostaining with anti-Spatial and anti-GFAP antibodies shows that Spatial does not colocalize with the GFAP astrocyte marker. The inset in E3 shows a high power view of the box. (F1-F3) A double immunostaining with anti-Spatial and anti-synaptophysin antibodies of the CA3 region shows that Spatial is present in some synaptic area. The inset in F3 shows a high power view of the box. (G1-G3) At P16 in the DG, Spatial is strongly detected in the external layer containing neurons under active differentiation (arrow) while no expression is detected in proliferating neurons of the internal layer (asterisk). (H1-H3) In the adult, Spatial continues to be expressed in the DG where neurogenesis persists. A DAPI counterstaining was used to visualize the structure of the DG. Scale bars in (A): 200 μm ; (B-C): 50 μm ; (D1-D3) and (F1-F3): 100 μm ; (E1-E3) upper panel: 20 μm ; lower panel: 5 μm ; (F1-F3): 20 μm ; (G1-G2): 100 μm ; (H1-H2): 50 μm .

Fig. 5- In primary cultures of hippocampal neurons Spatial displays a somatodendritic pattern and it is present in some synaptic regions. (A1-A3) A co-immunostaining with anti-Spatial and anti-MAP2 antibodies shows that Spatial strongly colocalizes with the MAP2 somatodendritic marker. (B1-B3) In contrast, co-immunostaining of Spatial and the axonal marker NF (SMI31) shows that Spatial is faintly detected in axonal processes of hippocampal neurons (arrow). The panel C exhibits a co-immunostaining of Spatial and the synaptic synaptophysin marker. (D1-D3) A high magnification shows that Spatial colocalizes in some synaptic areas (arrows). Scale bars in (A-C): 10 μm ; (D): 5 μm .

Fig. 6- Spatial interacts with the kinesin-motor KIF17. (A) Spatial co-immunoprecipitates with KIF17. (Left panel) The Spatial-KIF17 complex was immunoprecipitated from mouse hippocampal lysates using anti-Spatial antibody. The complex precipitated contained both Spatial- ϵ , - β and KIF17 as assessed by immunoblotting with anti-KIF17 and anti-Spatial antibodies respectively. (Right Panel) A reverse co-immunoprecipitation of endogenous KIF17 shows its association with Spatial through Spatial- ϵ and - β as assessed by IB with anti-KIF17 and anti-Spatial antibodies, respectively. In contrast, rabbit IgG did not pull down these proteins.

Molecular weight markers are shown to the left of the blots. Asterisks indicate heavy-chain immunoglobulins. (B) Spatial colocalizes with the kinesin-motor KIF17. After 15 days of culture, hippocampal neurons were co-immunostained with anti-Spatial and anti-KIF17 antibodies. Nuclei cells are visualized by a DAPI counterstaining. The lower panel represents a higher magnification showing the colocalization of Spatial and KIF17 in the same vesicles (arrowheads). (C-D) Spatial colocalizes with KIF17 in the adult mouse brain. High magnifications of the hippocampal CA3 region (C) and cerebral cortex (D) co-immunostained with anti-Spatial and anti-KIF17 antibodies are shown. Nuclei cells are visualized by a DAPI counterstaining (blue). Arrowheads indicate the colocalization of Spatial and KIF17 in the same vesicles inside the cell body. Scale bars in (B), upper panel: 10 μm ; lower panel: 2 μm ; (C): 7 μm ; (D): 10 μm .

Supplementary Fig. 1- Quantitative analysis of the expression of Spatial- ϵ and - β proteins during mouse cerebellar development. We quantified using the Image J software the expression of Spatial- ϵ and - β proteins normalized to the β -actin used as a loading control in the Western-blot shown in Fig. 1I. Spatial- ϵ and - β exhibit a differential expression characterized by a late expression of Spatial- β detectable at P4 in contrast to Spatial- ϵ which is expressed earlier.

Supplementary Fig. 2- In the adult neocortex, Spatial was also detected by ISH (A, B) and immunofluorescence (C, D) analyses. We observed on these brain sagittal sections a strong expression of Spatial restricted to large pyramidal neurons in layer III. (D) A higher magnification of the box in C shows that Spatial is localized in the cytoplasm of these cells. Scale bars (A): 400 μm ; (B): 200 μm ; (C): 150 μm ; (D): 50 μm .

References

1. Mentlein, R., and Kendall, M. D. (2000). The brain and thymus have much in common: a functional analysis of their microenvironments. *Immunol Today* **21**, 133-40.
2. Flomerfelt, F. A., Kim, M. G., and Schwartz, R. H. (2000). Spatial, a gene expressed in thymic stromal cells, depends on three-dimensional thymus organization for its expression. *Genes Immun* **1**, 391-401.

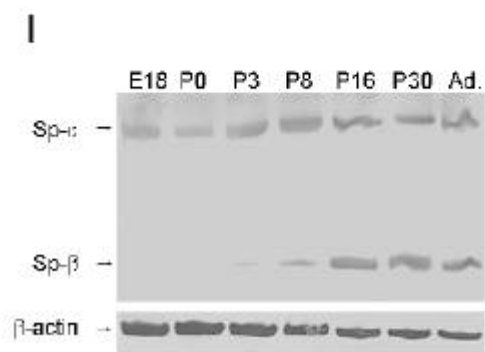
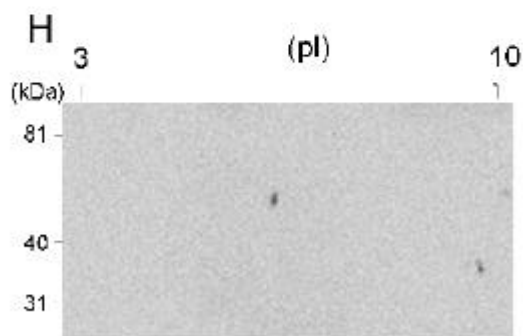
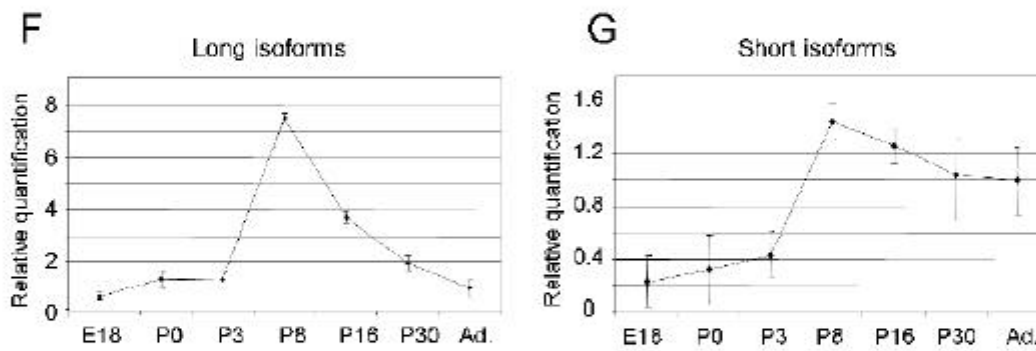
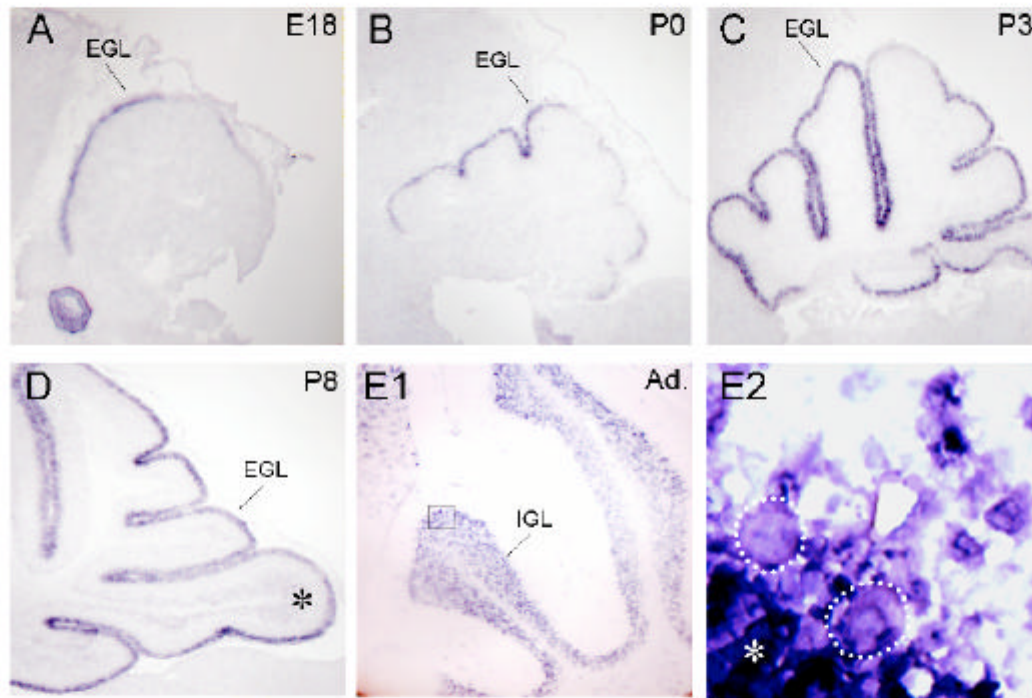
3. Irla, M., Puthier, D., Granjeaud, S., Saade, M., Victorero, G., Mattei, M. G., and Nguyen, C. (2004). Genomic organization and the tissue distribution of alternatively spliced isoforms of the mouse Spatial gene. *BMC Genomics* **5**, 41.
4. Irla, M., Puthier, D., Le Goffic, R., Victorero, G., Freeman, T., Naquet, P., Samson, M., and Nguyen, C. (2003). Spatial, a new nuclear factor tightly regulated during mouse spermatogenesis. *Gene Expr Patterns* **3**, 135-8.
5. Saade, M., Irla, M., Govin, J., Victorero, G., Samson, M., and Nguyen, C. (2007). Dynamic distribution of Spatial during mouse spermatogenesis and its interaction with the kinesin KIF17b. *Exp Cell Res* **313**, 614-26.
6. Macho, B., Brancorsini, S., Fimia, G. M., Setou, M., Hirokawa, N., and Sassone-Corsi, P. (2002). CREM-dependent transcription in male germ cells controlled by a kinesin. *Science* **298**, 2388-90.
7. Jenkins, P. M., Hurd, T. W., Zhang, L., McEwen, D. P., Brown, R. L., Margolis, B., Verhey, K. J., and Martens, J. R. (2006). Ciliary targeting of olfactory CNG channels requires the CNGB1b subunit and the kinesin-2 motor protein, KIF17. *Curr Biol* **16**, 1211-6.
8. Chu, P. J., Rivera, J. F., and Arnold, D. B. (2006). A role for Kif17 in transport of Kv4.2. *J Biol Chem* **281**, 365-73.
9. Setou, M., Nakagawa, T., Seog, D. H., and Hirokawa, N. (2000). Kinesin superfamily motor protein KIF17 and mLin-10 in NMDA receptor-containing vesicle transport. *Science* **288**, 1796-802.
10. Chennathukuzhi, V., Morales, C. R., El-Alfy, M., and Hecht, N. B. (2003). The kinesin KIF17b and RNA-binding protein TB-RBP transport specific cAMP-responsive element modulator-regulated mRNAs in male germ cells. *Proc Natl Acad Sci U S A* **100**, 15566-71.
11. Dahmane, N., and Ruiz-i-Altaba, A. (1999). Sonic hedgehog regulates the growth and patterning of the cerebellum. *Development* **126**, 3089-100.
12. Livak, K. J., and Schmittgen, T. D. (2001). Analysis of relative gene expression data using real-time quantitative PCR and the 2(-Delta Delta C(T)) Method. *Methods* **25**, 402-8.
13. Laemmli, U. K. (1970). Cleavage of structural proteins during the assembly of the

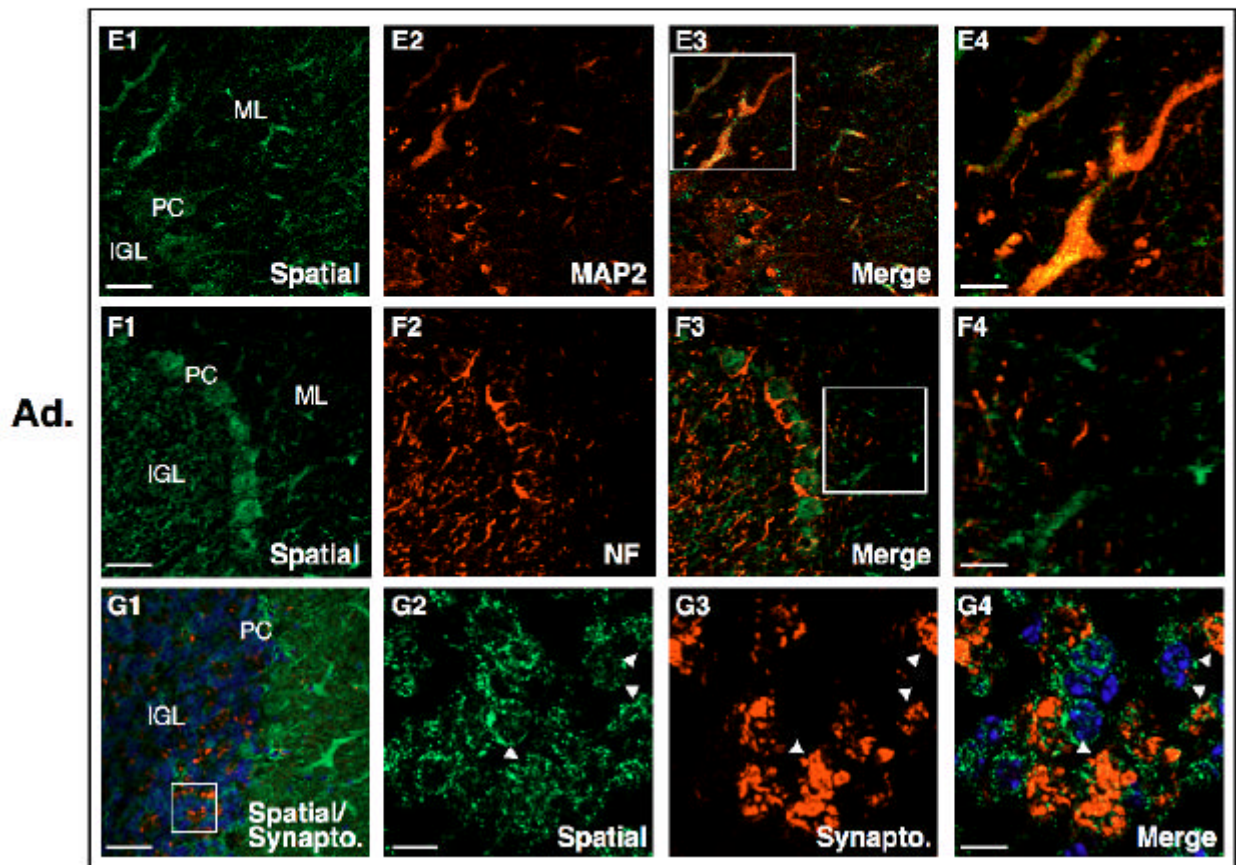
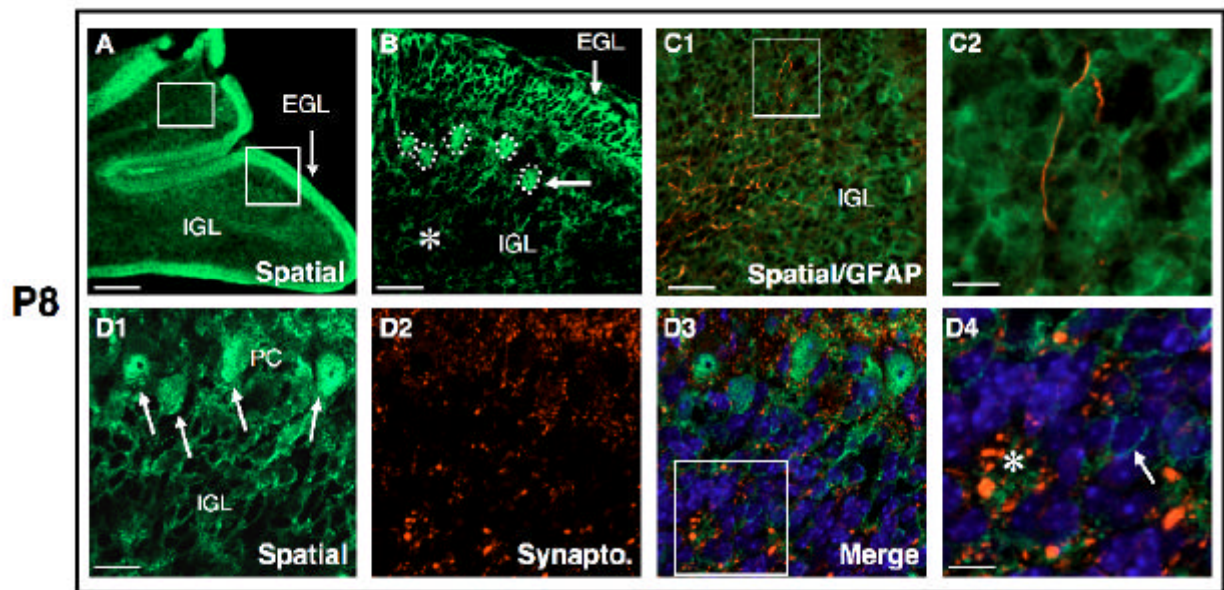
head of bacteriophage T4. *Nature* **227**, 680-5.

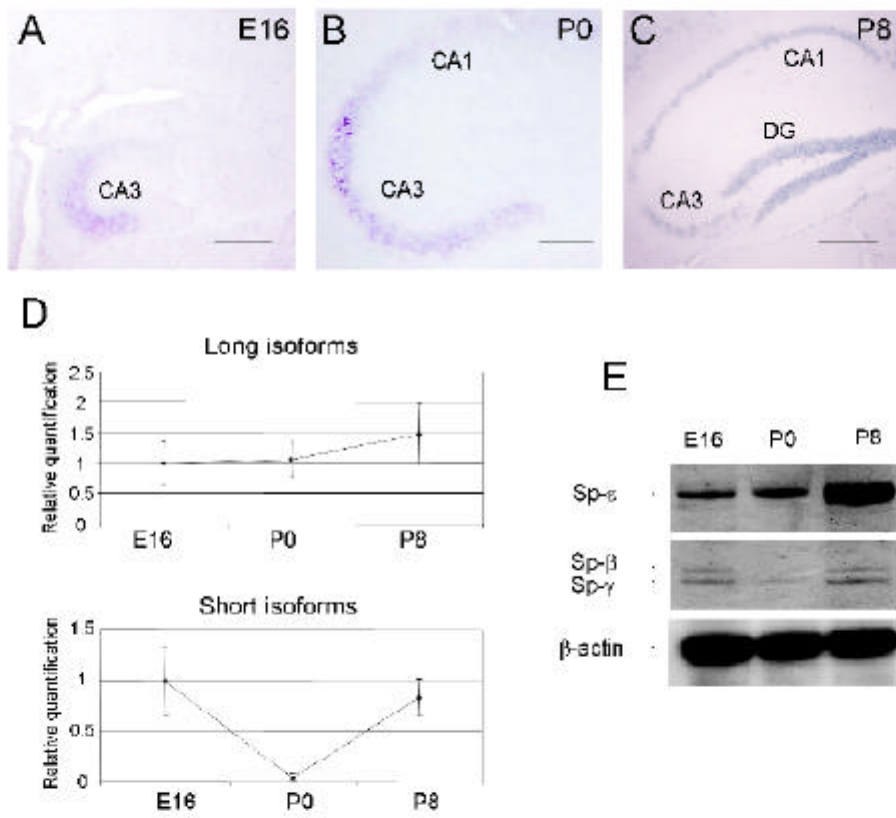
14. Sudhof, T. C., and Jahn, R. (1991). Proteins of synaptic vesicles involved in exocytosis and membrane recycling. *Neuron* **6**, 665-77.
15. Vale, R. D. (2003). The molecular motor toolbox for intracellular transport. *Cell* **112**, 467-80.
16. Hirokawa, N., and Takemura, R. (2005). Molecular motors and mechanisms of directional transport in neurons. *Nat Rev Neurosci* **6**, 201-14.
17. Kagami, Y., and Furuichi, T. (2001). Investigation of differentially expressed genes during the development of mouse cerebellum. *Brain Res Gene Expr Patterns* **1**, 39-59.
18. Jankowski, J., Holst, M. I., Liebig, C., Oberdick, J., and Baader, S. L. (2004). Engrailed-2 negatively regulates the onset of perinatal Purkinje cell differentiation. *J Comp Neurol* **472**, 87-99.
19. Stanfield, B. B., and Cowan, W. M. (1979). The development of the hippocampus and dentate gyrus in normal and reeler mice. *J Comp Neurol* **185**, 423-59.
20. Abrous, D. N., Koehl, M., and Le Moal, M. (2005). Adult neurogenesis: from precursors to network and physiology. *Physiol Rev* **85**, 523-69.
21. Krucker, T., Siggins, G. R., and Halpain, S. (2000). Dynamic actin filaments are required for stable long-term potentiation (LTP) in area CA1 of the hippocampus. *Proc Natl Acad Sci U S A* **97**, 6856-61.
22. Matsuzaki, M., Honkura, N., Ellis-Davies, G. C., and Kasai, H. (2004). Structural basis of long-term potentiation in single dendritic spines. *Nature* **429**, 761-6.
23. Hirokawa, N., and Takemura, R. (2004). Kinesin superfamily proteins and their various functions and dynamics. *Exp Cell Res* **301**, 50-9.
24. Wang, H., Ferguson, G. D., Pineda, V. V., Cundiff, P. E., and Storm, D. R. (2004). Overexpression of type-1 adenylyl cyclase in mouse forebrain enhances recognition memory and LTP. *Nat Neurosci* **7**, 635-42.
25. Kayadjanian, N., Lee, H. S., Pina-Crespo, J., and Heinemann, S. F. (2007). Localization of glutamate receptors to distal dendrites depends on subunit composition and the kinesin motor protein KIF17. *Mol Cell Neurosci* **34**, 219-30.

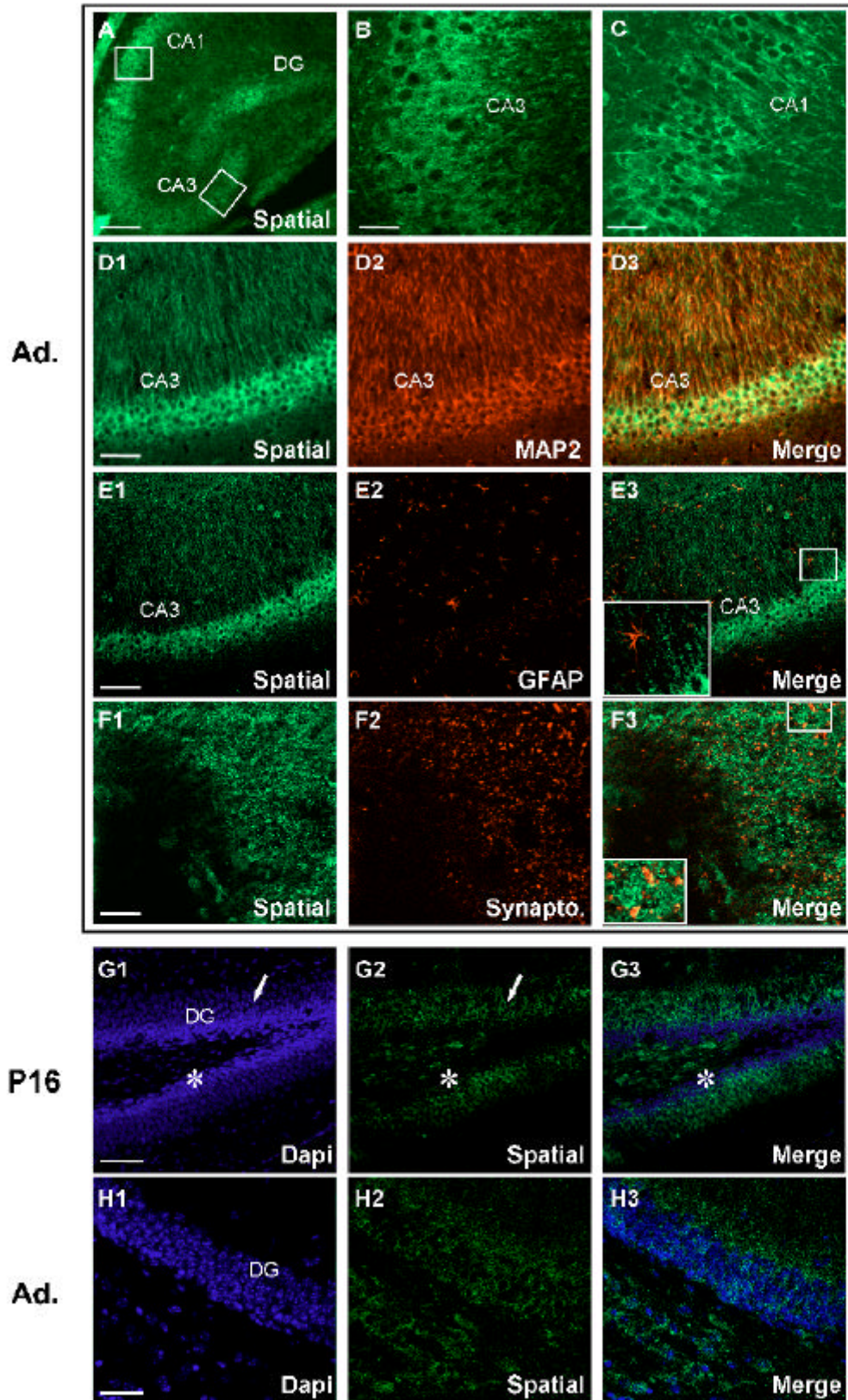
26. Guillaud L., Setou M., and Hirokawa N. (2003). KIF17 dynamics and regulation of NR2B trafficking in hippocampal neurons. *J. Neurosci.* **23**, 131-140.

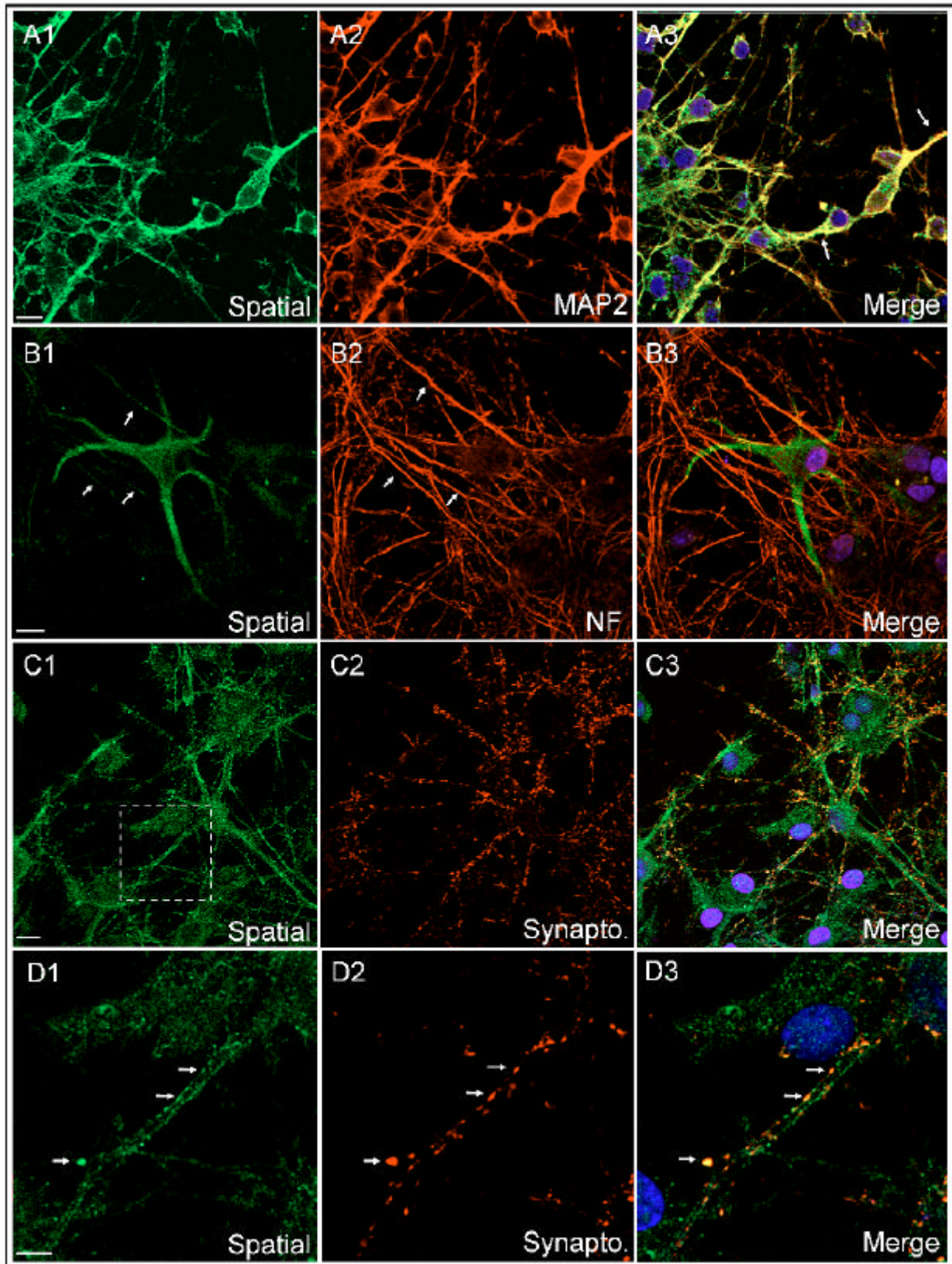
ACCEPTED MANUSCRIPT

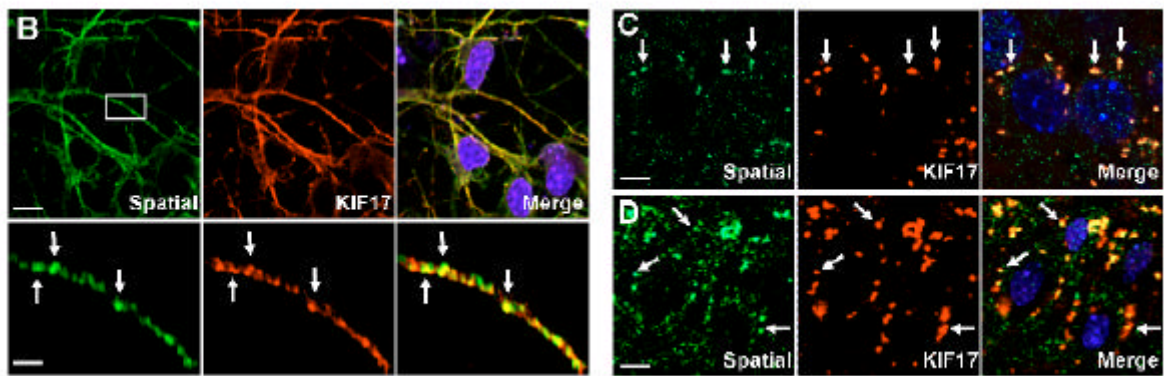
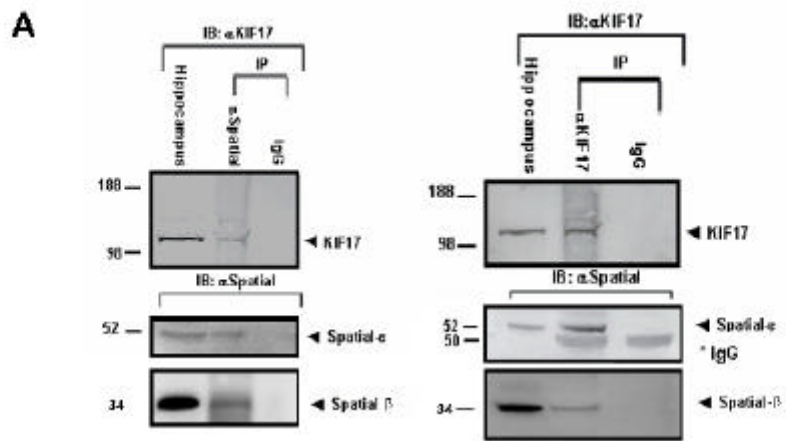












ACCEPTED